Available online at www.sciencedirect.com

jmr&t Journal of Materials Research and Technology

journal homepage: www.elsevier.com/locate/jmrt

Original Article

Crystal stabilization of α-$FAPbI_3$ perovskite by rapid annealing method in industrial scale

Govindhasamy Murugadoss [a,*], *Prabhakarn Arunachalam* [b], *Subhendu K. Panda* [c], *Manavalan Rajesh Kumar* [d], *Jothi Ramalingam Rajabathar* [b,**], *Hamad Al-Lohedan* [b], *M.D. Wasmiah* [b]

[a] *Centre for Nanoscience and Nanotechnology, Sathyabama Institute of Science and Technology, Chennai 600119, India*

[b] *Chemistry Department, College of Science, King Saud University, Riyadh, 11451, Saudi Arabia*

[c] *EMF Division, CSIR- Central Electrochemical Research Institute (CSIR-CECRI), Karaikudi, 630003, India*

[d] *Institute of Natural Science and Mathematics, Ural Federal University, Yekaterinburg, 620002, Russia*

ARTICLE INFO

Article history:
Received 26 November 2020
Accepted 29 March 2021
Available online 8 April 2021

Keywords:
α-$FAPbI_3$
Phase change/stability
Microstructure
Rapid annealing
X-ray techniques

ABSTRACT

Organic-inorganic hybrid formamidinium lead iodide ($FAPbI_3$) perovskite has shown tremendous attention in recently developed photovoltaics and optelectronic devices. However, it suffers from structural instability complications, particularly the spontaneous phase transition from a dark color photoactive perovskite phase (α-$FAPbI_3$) to a yellow color photo-inactive phase (δ-$FAPbI_3$) at room temperature. To stabilize the photoactive α-$FAPbI_3$, several methods were employed, including compositional engineering, 2D layer deposition on the surface, and solvent engineering method. In this communication, we have proposed a facile sequential rapid annealing method to produce the photoactive α-$FAPbI_3$ perovskite on an industrial scale, which is highly stable at room temperature. The structural, morphological, compositional, and optical properties of the perovskite were studied using X-ray diffraction (XRD), UV–visible absorption, Laser Raman, thermogravimetric analysis (TGA), and field emission electron microscopy with elemental analysis (FE-SEM & EDAX). The strong characteristic diffraction peaks of cubic structure in XRD showed the proposed additives free preparation method is more adaptable for the preparation of high quality α-$FAPbI_3$ perovskite for optoelectronic applications.

1. Introduction

The organic-inorganic hybrid perovskite solar cells (PSCs) have fascinated extensive attention due to their continuous increase in performance in a short period, and recently certified maximum power conversion efficiency (PCE) has reached up to 25.2% [1,2]. Such an excellent development is due to the very narrow bandgap, the long charge carrier diffusion length and high absorption coefficient, and the

* Corresponding author.
** Corresponding author.
E-mail addresses: murugadoss_g@yahoo.com (G. Murugadoss), jrajabathar@ksu.edu.sa (J.R. Rajabathar).

https://doi.org/10.1016/j.jmrt.2021.03.107

advantages of easy solution processing of perovskite materials to devices [3–5]. Among the existing organic-inorganic hybrid perovskites, the formamidinium lead iodide ($FAPbI_3$) perovskite has attracted significant attention because of numerous advantages such as larger and thermally stable organic formamidinium (FA) cation which can substitute the unstable methylammonium (MA) cation, the narrow bandgap of $FAPbI_3$ permits for near-infrared absorption, and $FAPbI_3$ has an elevated decomposition temperature. The $FAPbI_3$ is the most capable perovskite material for high-efficiency solar cells due to its tunable bandgap (1.5–1.4 eV), low exciton binding energy (<50 mV), high absorption coefficient in the range of 10^4–10^5 cm^{-1}, and long diffusion length of charge carrier (0.1–1.0 μm) [6,7].

Even though methylammonium lead iodide ($MAPbI_3$; $CH_3NH_3PbI_3$) is the widely explored hybrid perovskite for solar cell uses [8–12], superior activity in terms of photovoltaic efficiency is found $FAPbI_3$ ($CH(NH_2)_2PbI_3$). This is owing both to a smaller bandgap of $FAPbI_3$ and to the fact that the FA^+ ion, despite a shorter electric dipole concerning MA^+, has a much greater quadrupole and quicker reorientation dynamics that better screen the photoexcited carriers, improving their lifetime [13]. Moreover, the $FAPbI_3$ has better stability than $MAPbI_3$ at high temperatures. However, it is challenging to prepare room temperature stable photoactive $FAPbI_3$ thin films or powders required for solar cells or optoelectronic applications. It obtained only the yellow phase (photoinactive phase) using the standard chemical methods. To date, most of the research efforts on FA-based perovskite materials emphases on the stabilization of α-FAPbI3 structure at a comparatively lower temperature.

In order to produce the photoactive α-$FAPbI_3$ perovskite structure, in this work, we have applied a facile method that rapid annealing process to fabricate the stable perovskite powder. Since the $FAPbI_3$ perovskite powders are well crystalline, it can be used for a long time in the laboratory for photovoltaic and optoelectronic applications. But the precursors (FA^+ and PbI_2) of the perovskites are not stable due to its hygroscopic nature. Interestingly, the perovskite powder preparation approach is more advantageous for reproducibility of solar cell activity than the precursors directly mixing method because the underlying non-stoichiometry of the subsequent perovskite film can be eluded [7]. For comparison purposes, the perovskites were prepared by one-step and two-step rapid annealing method and then evaluated the phase changes, microstructural variation, and optical bandgap modification.

2. Experimental method

2.1. Chemicals

Lead (II) iodide 99% (PbI_2), hydroiodic acid (HI), formamidine acetate, hydroiodic acid (HI), chlorobenzene (CB) and

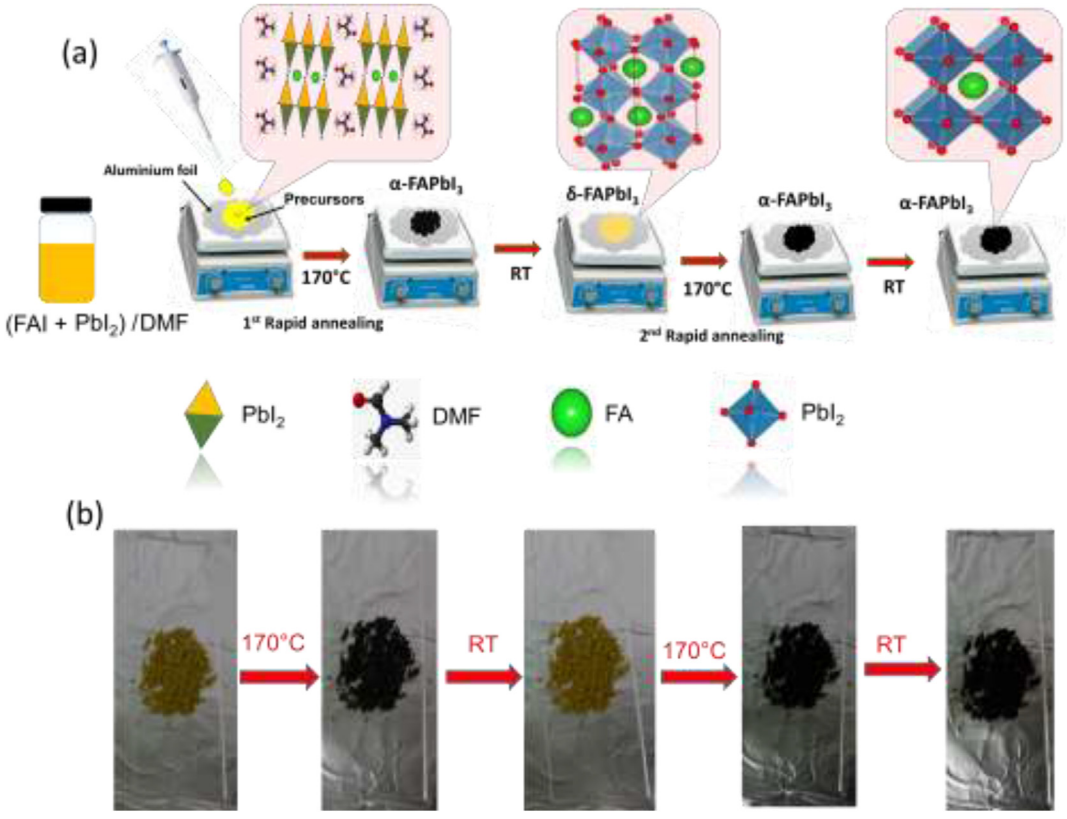

Fig. 1 – (a) Schematic representation of α-$FAPbI_3$ phase stabilization process by rapid annealing method, (b) Perovskite powder color variation before and after sintering.

dimethylformamide were acquired from Sigma–Aldrich and used as received.

2.2. Synthesis of formamidinium iodide ($CH(NH_2)_2I$)

Formamidinium iodide (FAI) crystals were obtained by reacting 5 g of formamidine acetate with 10 ml HI in a beaker at 0 °C for 2 h with vigorous stirring. The colloidal solution with brown color crystals was then washed using diethyl ether several times until the crystals become bright white. After that, the solution was vacuum evaporated at 100 °C for 24 at ambient conditions.

2.3. $FAPbI_3$ perovskites preparation

The sample preparation method is schematically demonstrated in Fig. 1(a). Typically, perovskite precursor was obtained by mixing of 1:1 M ratio of FAI and PbI_2 in N, N-dimethylmethanamide (DMF) solvent. At the first step, the perovskite solution was slowly dropped on the aluminium foil surface, which was kept on a hot plate at 170 °C for 5 min. When dropped on the hot aluminium foil, the yellow color solution was rapidly turned into dark color powder by evaporation of the solvents, indicating the formation of α-$FAPbI_3$ perovskite. After 5 min, when the aluminium foil was suddenly cooled down to room temperature by taking it out from the hot plate, the dark colour turns back to yellow colour powder within a few minutes. Subsequently, in the second step, the yellow color powder was again annealed on the aluminium foil surface over the hot plate (at 170 °C) for 10 min. Then, the sample was removed from the hot plate and placed at room temperature. For comparison, we have prepared two samples, one from the one-step method and another from the two-step method. Then, the two samples were characterized by various characterization techniques.

2.4. Characterization

X-ray diffraction (XRD, PW3040/60 X'pert PRD) for the perovskites was studied using Cu-Kα radiation (λ = 0.1540 nm). Raman spectra were measured using Lab RAM HR Evolution Laser-Raman spectrometer with an excitation wavelength of 514 nm. UV–Vis diffuse reflectance spectra were performed using a UV/VIS-NIR double beam spectrophotometer (VARIAN, Cary 5000). TGA analysis was conducted using TG-DTA, SQT Q600 model. The microstructure of perovskite powders and elemental composition were characterized using FE-SEM (Hitachi, S-4800, Japan). The high-resolution transmission electron microscopy (HR-TEM) was executed using Tecnai F20 G2 operated at 200 kV to evaluate structural and morphological information. For HR-TEM analysis, the powder samples were well dispersed into the CB and then drop-cast on the gold grid. In order to vaporize the solvents, the sample grid was light irradiated using sodium lamb.

3. Results and discussion

As seen in Fig. 1(b), the photocopy of perovskite powder color was significantly changed into yellow-to-dark under heating at 170 °C in air atmosphere; subsequently, the dark color was reverted at room temperature, in continue to the two-step rapid annealing method, the powder samples stand with dark color even after cooling to room temperature. The noticeable structural changes were further confirmed by XRD. The XRD spectrum of the perovskite sample was measured after 4 weeks. Surprisingly, the dark color of the sample was maintained for 2 weeks, it clearly showed that the α-$FAPbI_3$ perovskite powder is stable for 4 weeks in ambient condition by preparing the two-step rapid annealing method. Fig. 2 shows XRD spectra of the $FAPbI_3$ powder samples prepared by one-step two-step rapid annealing method at 170 °C and 4 weeks aged sample. In the one-step method, the perovskite precursor was rapidly annealed, then the resultant powder sample was kept down to natural circumstances, and the sample was directly measured XRD. The perovskite powder prepared by the one step-method was again subjected to rapid annealing at 170 °C and then cooled to the two-step method's temperature. The resultant dark colour powder was used to carry out the XRD and other characterization studies. The XRD pattern of the yellow-coloured perovskite prepared by the one-step method showed as absolutely photo-inactive (hexagonal δ-$FAPbI_3$) [14]. At room temperature, the black α-$FAPbI_3$ instinctively changes to a more stable yellow δ-$FAPbI_3$. However, the δ-$FAPbI_3$ was completely disappeared when the sample was again subjected to a rapid annealing process. The most intense diffraction peak positioned at 13.9° agrees to (0 0 1) diffraction planes and the peaks situated at 19.8°, 24.3°, 28.1°, 31.4°, 34.6°, 40.1° and 42.7° are related to (0 1 1) (1 1 1) (0 0 2) (0 1 2) (1 1 2) (0 2 2) and (0 3 3) diffraction planes correspond to the cubic structure of α-$FAPbI_3$ [15]. The sharp diffraction peaks specify the high crystallinity of the α-$FAPbI_3$ perovskite. Interestingly, the α-$FAPbI_3$ perovskite prepared by the two-step method showed long-time stability at room temperature. Fig. 2 shows the XRD pattern of the 4 weeks aged perovskite, which is prepared by a two-step rapid annealing method. The appeared diffraction planes are corresponding to

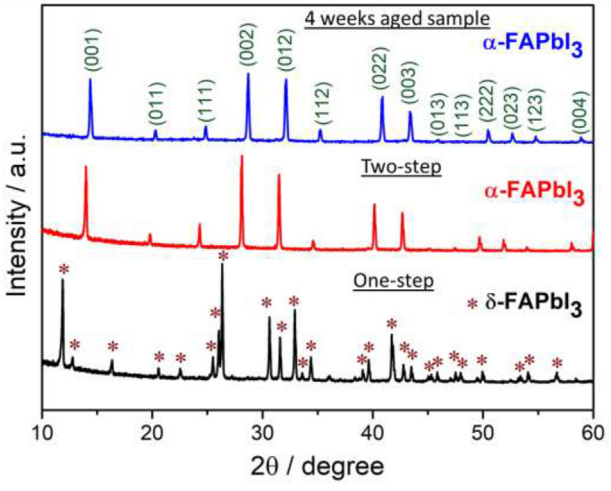

Fig. 2 – X-ray diffraction patterns of the perovskites prepared by one-step (δ-$FAPbI_3$), two-step (α-$FAPbI_3$) rapid annealing method and 4 weeks aged α-$FAPbI_3$ perovskite prepared by two-step process.

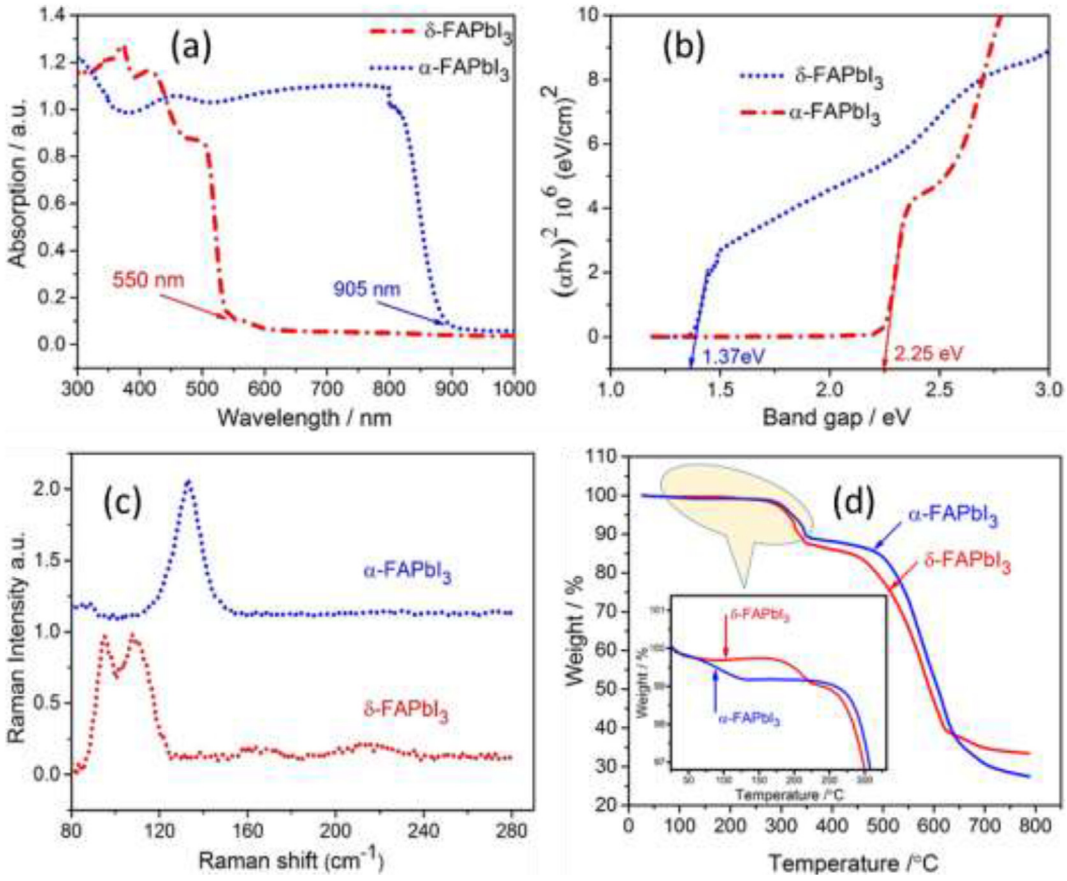

Fig. 3 – (a–d) UV–vis absorption spectra, bandgap curves, Laser Raman, and TG-DTA curves of perovskites were prepared by one-step (δ-$FAPbI_3$) and two-step (α-$FAPbI_3$) rapid annealing methods.

α-$FAPbI_3$. No impurity or secondary peaks related to δ-$FAPbI_3$ were detected, it shows high stability of the perovskite. The increasing stability is due to the perovskite's high crystallinity by the rapid crystallization process with reducing grain boundaries.

To investigate this exciting modification in the XRD patterns by one-step and two-step annealing, UV–Vis absorption spectra from both the powder samples were studied, and the results are presented in Fig. 3(a). The absorption edge shifted from 550 nm (for δ-$FAPbI_3$) to 905 nm (α-$FAPbI_3$ phase) for the one-step and two-step method, respectively. The optical absorption of α-$FAPbI_3$is covered the entire visible as well as near the IR region. The optical band gaps assessed from the equivalent Tauc plots (Fig. 3(b)), it showed the values of 2.25 eV and 1.37 eV for δ-$FAPbI_3$ and α-$FAPbI_3$, respectively, which is in good consistent with earlier reports [16].

The Raman spectra for both the perovskites prepared by one-step and two-step methods performed at room temperature and the obtained result are presented in Fig. 3(c). The δ-phase in Fig. 3(c) exhibits two strong Raman modes cantered at 108 cm^{-1} with a low-energy peak at 94 cm^{-1} [17]. For a two-step annealed sample, a strong red-shifted peak at 133.5 cm^{-1} is indicative of the in-plane vibration of cubic α-phase $FAPbI_3$ [17].

TGA is employed to investigate the thermal stability for the powder samples, and the obtained results are given in Fig. 3(d). The TG-study was performed at a nitrogen atmosphere with a temperature increment of 10 °C/min. No drastic changes were observed from the room temperature to 200 °C for both samples. The small weight loss (>1%) for the α-$FAPbI_3$ (see magnified curve) may be due to the evaporation of the atmospheric moisture. Surprisingly, the α-$FAPbI_3$ perovskite showed high thermal stability (>250 °C) but the δ-$FAPbI_3$ perovskite the decomposition started from around 180 °C. From the thermal study results, it is clearly observed that the α-$FAPbI_3$ perovskite is having high thermal stability than the δ-$FAPbI_3$ perovskite.

In order to understand the morphological changes with respect to the rapid annealing process, the structures of the samples were investigated by FE-SEM. Fig. 4(a–c) shows FE-SEM images of the δ-$FAPbI_3$ perovskite with different magnifications. The FE-SEM images are displayed the rod-like structure of the perovskite. However, the rod structure was wholly transformed into microstructures crystals when used the rapid annealed two-step process, as shown in Fig. 4(e–g). The observed morphology changes are further confirmed the structural changes from δ to α phase of the perovskite by the successive rapid thermal annealing

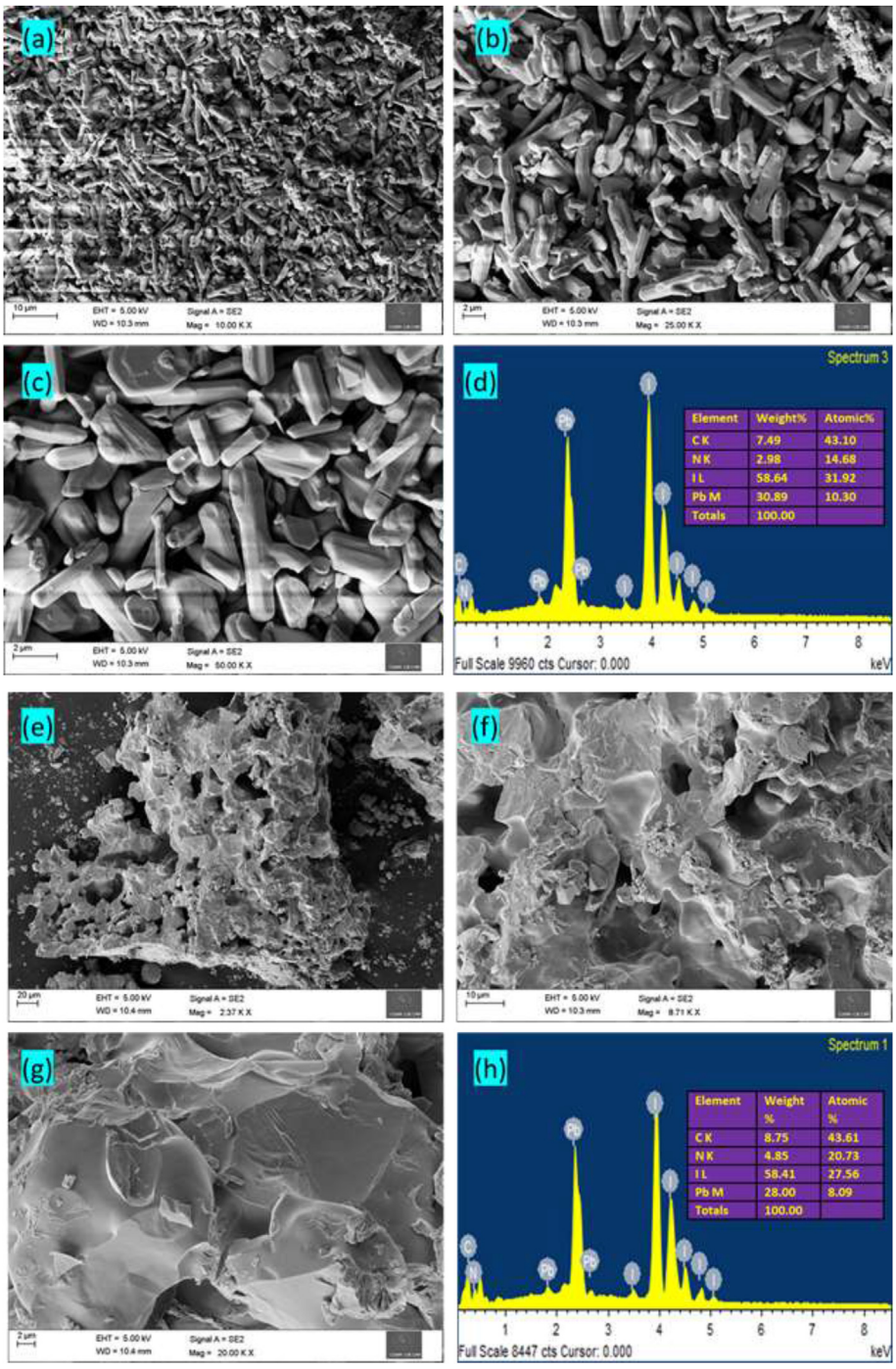

Fig. 4 – (a–d) FE-SEM images of δ-$FAPbI_3$ with different magnifications and EDAX spectrum (e–h) Micrograph images of various magnifications of α-$FAPbI_3$ perovskite and corresponding EDAX result.

process. Along with the phase change, the reduction in grain boundaries in the powder sample of α-$FAPbI_3$ may provide improved stability without modifying its composition. The elemental composition of the perovskite studied by EDAX analysis as showed in Fig. 4(d) and (h) for δ-$FAPbI_3$ and α-$FAPbI_3$, respectively. The dramatic changes in the perovskites' structural and morphological changes are mainly due to the variation of the I/Pb ratio [18]. The calculated ratio of I to Pb is 3.10 and 3.41 for δ-$FAPbI_3$ and α-$FAPbI_3$, respectively.

To further investigate morphological and structural information of the perovskites, HR-TEM was performed. As seen in Fig. 5(a–f), fragmented pieces of rods showed with tiny particles spread over the nods. The rod-like structure is in good agreement with FE-SEM images. The high magnified images (Fig. 5(e–f)) clearly show that the rod structure is formed by the tiny particles assembled. The selected area electron diffraction (SAED) pattern of the δ-phase perovskite showed a distinguished spot on a pattern. It clearly indicates a well crystalline hexagonal

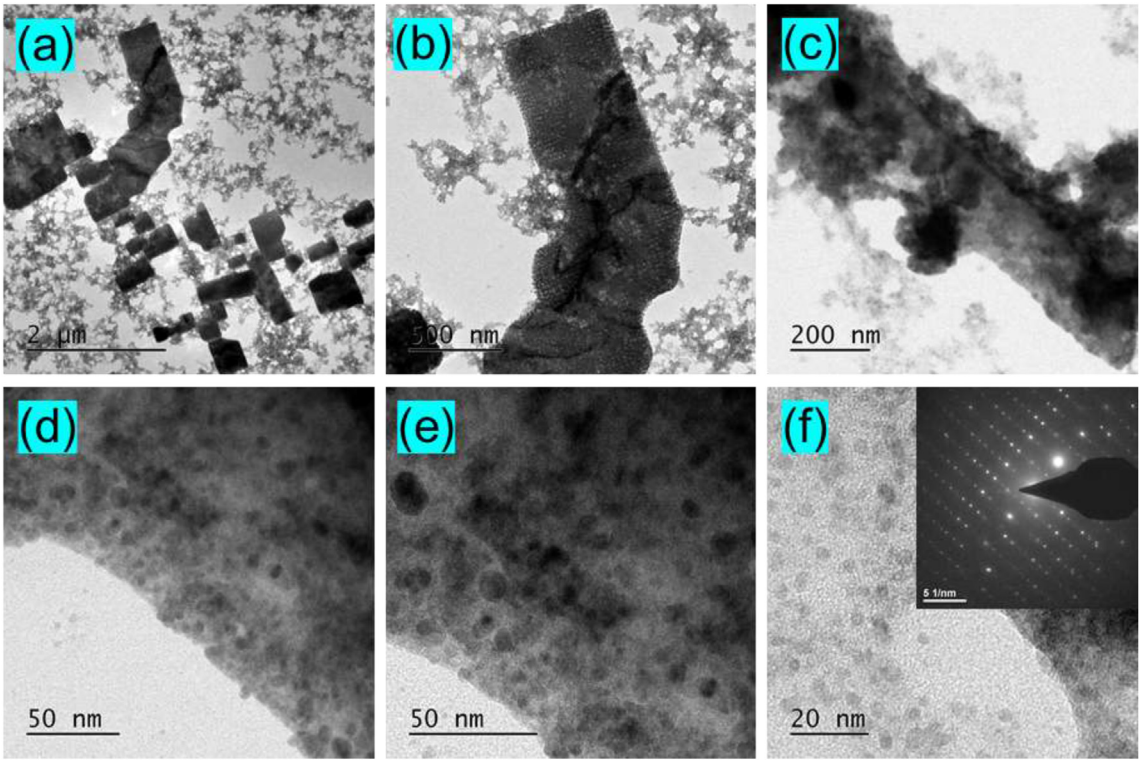

Fig. 5 – (a–f) HR-TEM images of δ-$FAPbI_3$ perovskite with different magnifications which prepared by the rapid annealed method. SAED pattern of the corresponding sample showed in inset image of (f).

crystal structure of the samples. Fig. 6(a–f) shows HR-TEM images of the α-$FAPbI_3$ perovskites with various magnifications. The perovskite images show larger crystals with random shapes due to the uncontrolled growth during the rapid annealing. The high-resolution HR-TEM image in Fig. 6(f) showed well-resolved springs. The d-spacing value

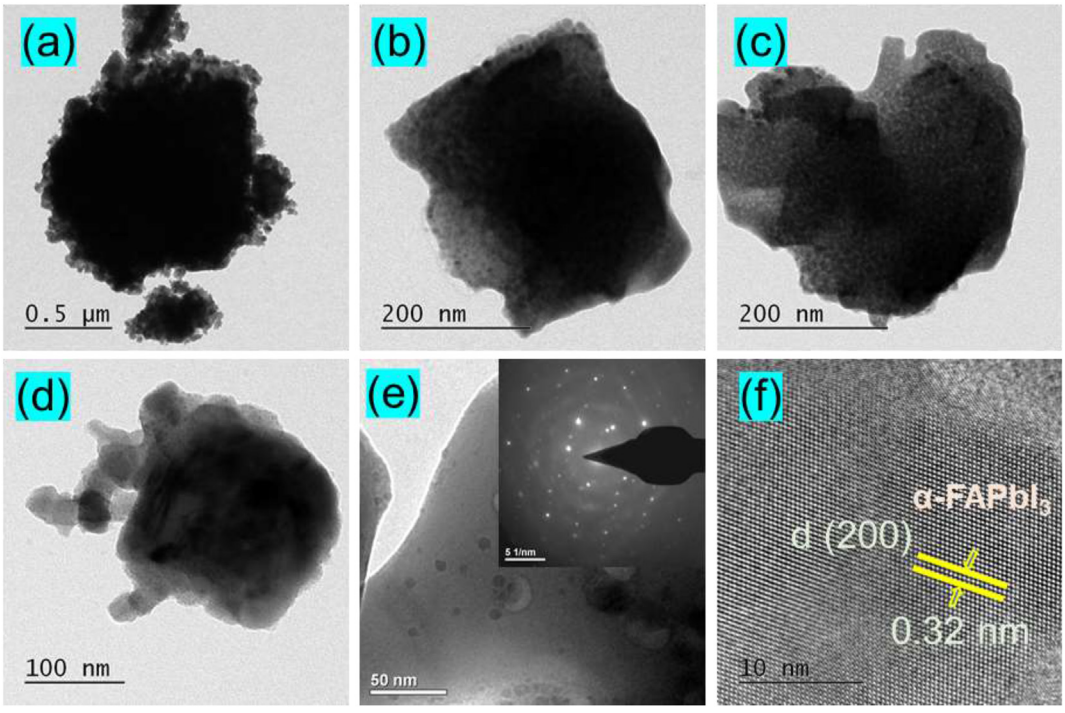

Fig. 6 – (a–f) HR-TEM images of α-$FAPbI_3$ perovskite with different magnifications. SAED pattern of the corresponding sample showed in inset image of (E).

of 0.32 nm of (2 0 0) plane confirms the cubic structure of the perovskite. The SAED pattern of the α-$FAPbI_3$ distinguished pattern confirms the high crystalline nature of the product by the rapid annealing method.

4. Conclusions

In summary, we have prepared a highly air-stable α-$FAPbI_3$ perovskite on an industrial scale by a facile, rapid annealing method without using any additives. The structural, morphology, and optical modifications with respect to the crystallization of $FAPbI_3$ are demonstrated. The changing optical absorption and morphology of the samples have clearly demonstrated that the high quality photoactive cubic structure formed by the rapid annealing method. The rod-like structure was dramatically changed into large grains when the powder annealed rapidly. The large crystals have ascribed the conversion of α to δ-phase. The remarkable method for preparing stable photoactive α-$FAPbI_3$ perovskite crystals reported here might encourage researchers to apply the perovskite for industrial-scale using a facile solution-processed for diverse applications.

Declaration of Competing Interest

The authors declare that they have no known competing financial interests or personal relationships that could have appeared to influence the work reported in this paper.

Acknowledgement

Dr. G. Murugadoss acknowledges to the management of Sathyabama Institute of Science and Technology, Chennai, Tamilnadu, India for provided lab facility. We extend their appreciation to the Deputyship for Research & Innovation, "Ministry of Education" in Saudi Arabia for funding this research work through the project no. (IFK-SURG-1440-014).

REFERENCES

[1] Kojima A, Teshima K, Shirai Y, Miyasaka T. J Am Chem Soc 2009;131:6050.
[2] National Renewable Energy Laboratory (NREL), Best Research-Cell Efficiencies, https://www.nrel.gov/pv/cell-efficiency.html, accessed: December, 2019.
[3] Wehrenfennig C, Eperon GE, Johnston MB, Snaith HJ, Herz LM. Adv Mater 2014;26:1584.
[4] Oga H, Saeki A, Ogomi Y, Hayase S, Seki S. J Am Chem Soc 2014;136:13818.
[5] Zhang W, Saliba M, Moore D, Pathak S, Hörantner MT, Stergiopoulos T, et al. Nat Commun 2015;6:6142.
[6] Lee J-W, Seol D-J, Cho A-N, Park N-G. Adv Mater 2014;26:4991.
[7] Zhang Y, Seo S, Lim SY, Kim Y, Kim SG, Lee DK, et al. ACS Energy Letters 2019;5:360.
[8] Murugadoss G, Kumar MR, Shanmugam VM. Mater. Sci. Semicond. Proc. 2020;117:105177.
[9] Kakavelakis G, Paradisanos I, Paci B, Generosi A, Papachatzakis M, Maksudov T, et al. Adv. Energy Mater. 2018;8:1702287.
[10] Murugadoss G, Thangamuthu R, Kumar SMS, Narayanasamy A, Kumar MR, Rathishkumar A. J Alloys Compd 2019;787:17.
[11] Murugadoss G, Thangamuthu R. Sol Energy 2019;179:151.
[12] Ogunniran KO, Murugadoss G, Thangamuthu R, Karthikayan J, Murugan P. Sol Energy Mater Sol Cell 2019;191:316.
[13] Chen T, Chen WL, Foley BJ, Lee J, Ruff JC, Ko JYP, et al. Proc Natl Acad Sci Unit States Am 2017;114:7519.
[14] Wang Z, Zhou Y, Pang S, Xiao Z, Zhang J, Chai W, et al. Chem Mater 2015;27:7149.
[15] Murugadoss G, Thangamuthu R, Kumar MR. Mater Lett 2018;231:16.
[16] Murugadoss G, Kuppusami P, Kumar MR. Inorg Chem Commun 2020;119:108059.
[17] Steele JA, Yuan H, Tan CYX, Keshavarz M, Steuwe C, Roeffaers MBJ, et al. ACS Nano 2017;11:8072.
[18] Cordero F, Craciun F, Trequattrini F, Generosi A, Paci B, Paoletti AM, et al. J Phys Chem Lett 2019;10:2463.